

A modelling study of the factors governing the convective boundary layer height over isolated mountain ridges

Stefano Serafin¹ and Stephan F.J. De Wekker²

¹ Department of Meteorology and Geophysics, University of Vienna, Vienna (Austria)

² Department of Environmental Sciences, University of Virginia, Charlottesville (VA, USA)

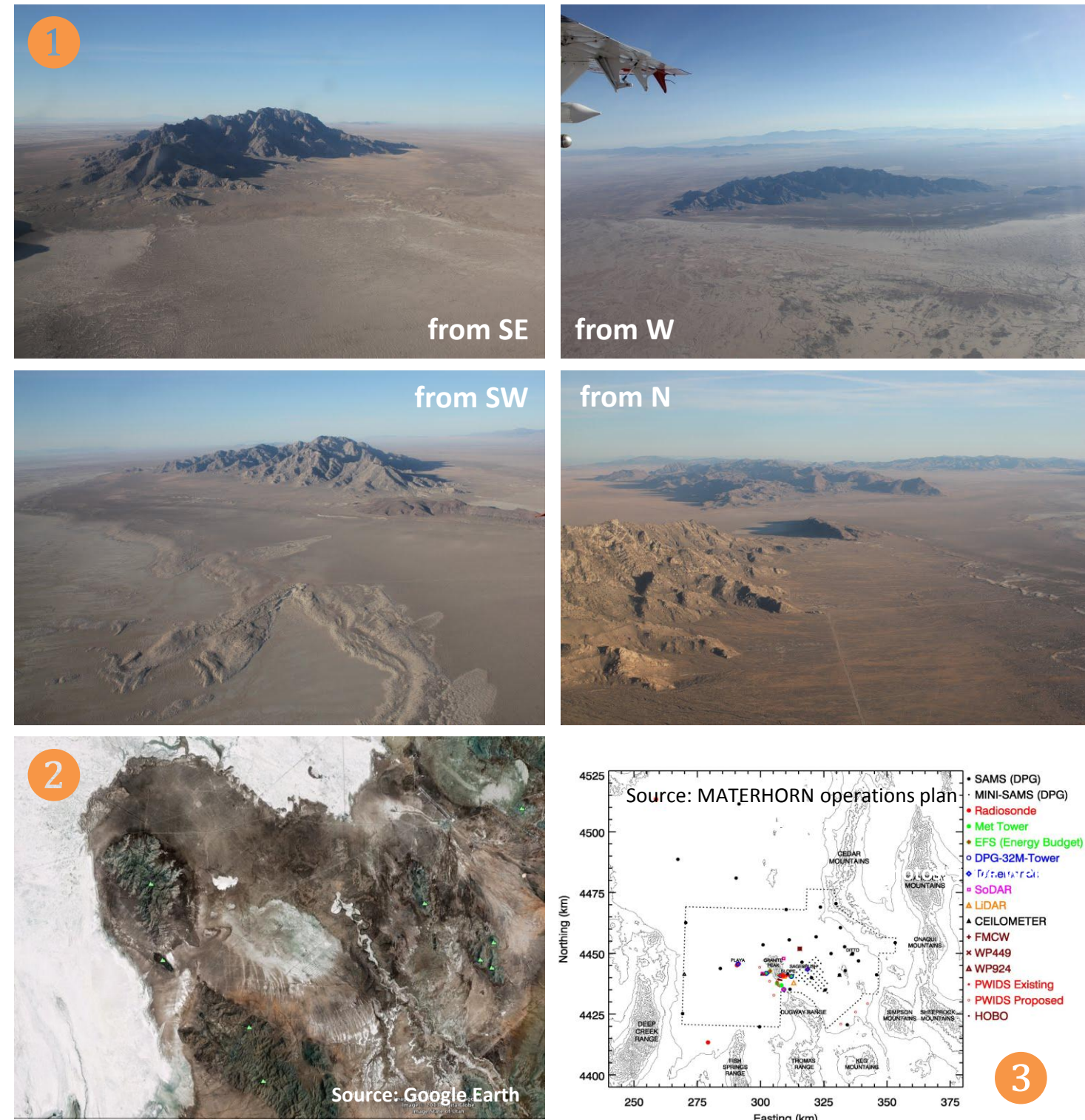
Introduction: Dugway Proving Ground, Granite Peak and the MATERHORN project

Granite Peak, located in the Dugway Proving Ground (DPG) in western Utah, is an isolated mountain rising ~800 m above the surrounding terrain (1). Granite Peak separates a salt flat (playa) to the W from a NW-sloping plain covered by herbaceous vegetation to the E (2).

During the day, thermally-driven flows induced both by topography and by land-surface heterogeneity are expected to occur in the area and to affect the CBL development.

During fall 2012 and spring 2013, DPG was the target area of the MATERHORN project. An existing meso-network of measurement stations (SAMS) was enhanced with an extensive set of special measurement platforms (3).

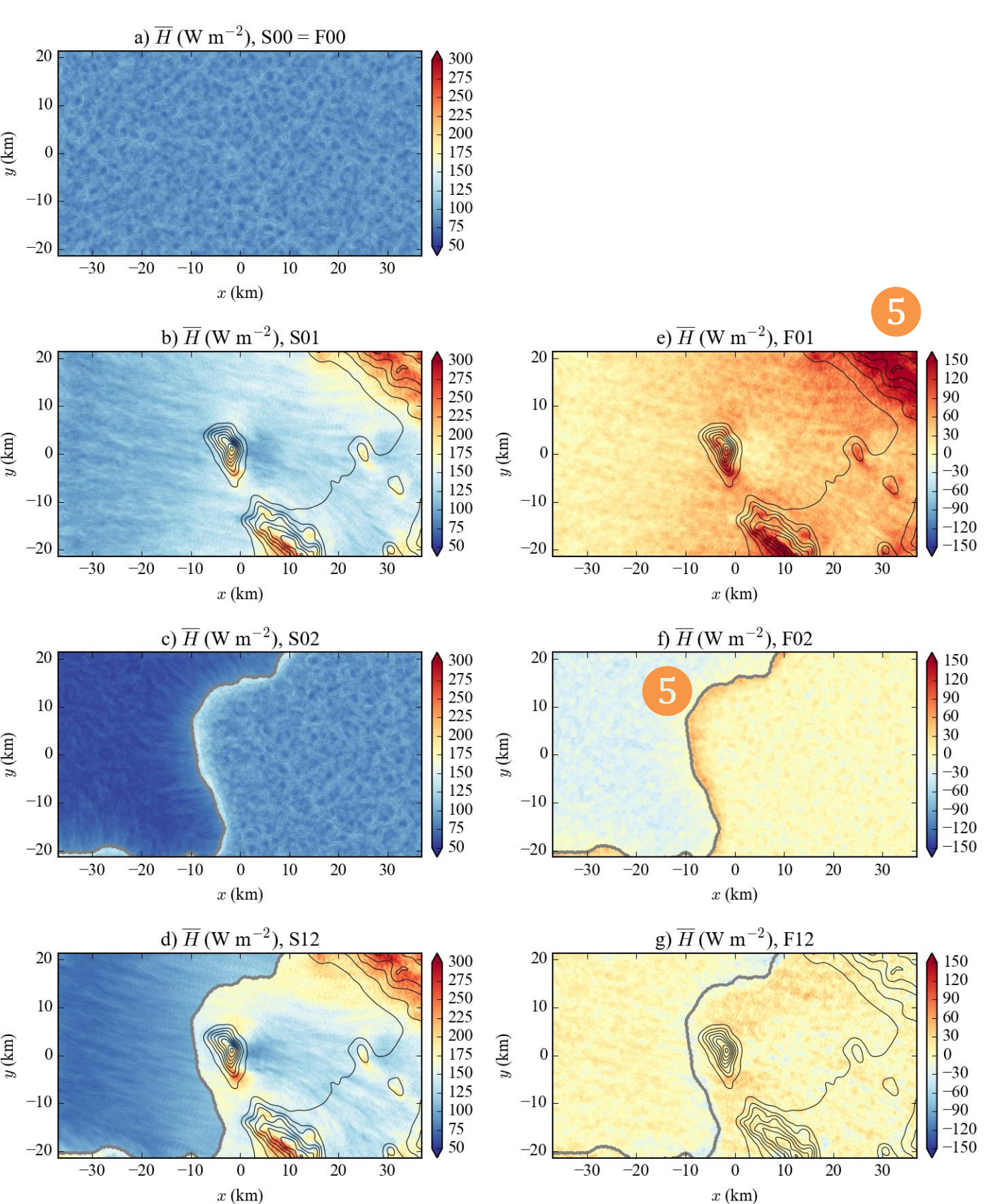
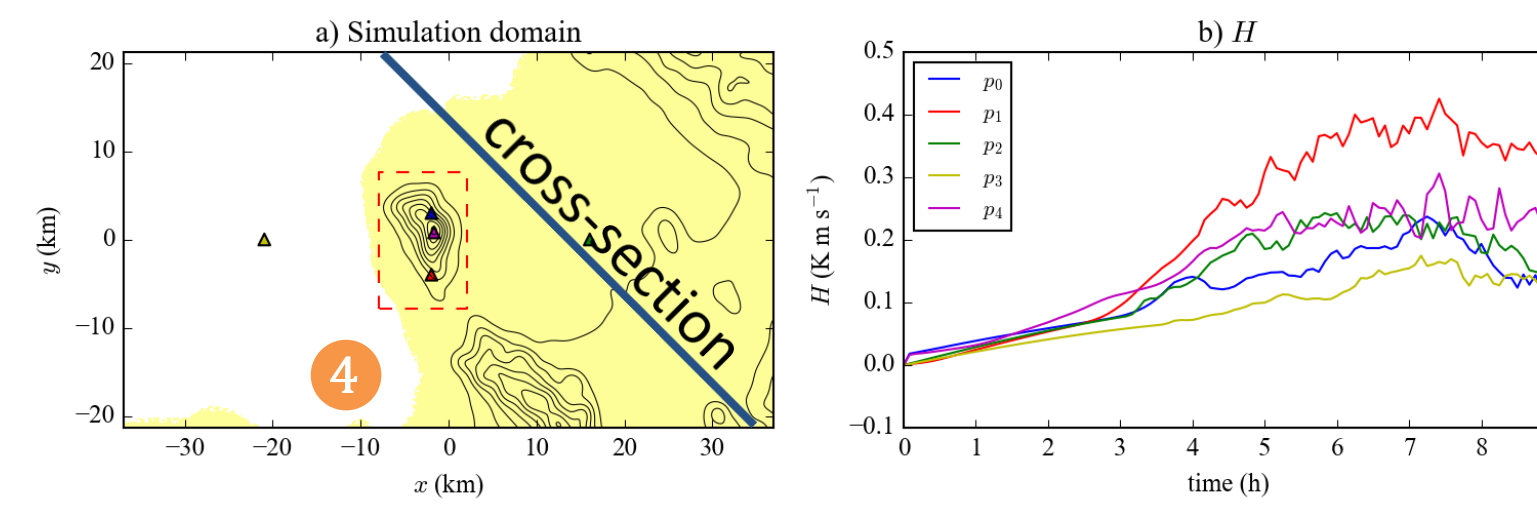
Our purpose: understand the mechanisms of CBL height variability at DPG.



CM1

Simulations presented in this study were performed using the CM1 model (Bryan and Fritsch, 2002).

- Topography from SRTM data at 1" resolution, resampled and low-pass filtered on the model grid.
- $\Delta x = 100$ m, 88 x 62 km domain.
- $\Delta z = 20$ m near the ground, constant stretching factor of ~5%, 80 levels, model top at 16000 m MSL.
- Height-based terrain-following coordinate system.
- Deardorff (1980) TKE-based SGS turbulence closure. 5th-order horizontal and vertical advection.
- Surface sensible heat flux imposed, with different intensity in two regions (playa/sagebrush plain 4).
- IC: quiescent atmosphere, thermal profile as on 10 October 2012 (MATERHORN IOP5).
- Rayleigh damping within 10 km from the lateral boundaries, open lateral boundary conditions.
- Rigid-lid model top, Rayleigh damping in the upper 5 km.
- Passive tracer injected at the surface on the playa side, with constant mass flux.
- Nine-hour simulations initialized at 6 LST.



Modelling the sensible heat flux at the surface

The (kinematic) sensible heat flux from the ground to the atmosphere is modelled with a bulk transfer relationship: $H = C_d U \Delta T$. Here, C_d is the drag coefficient, U the 10-m wind speed and ΔT the temperature difference between the ground and the atmosphere.

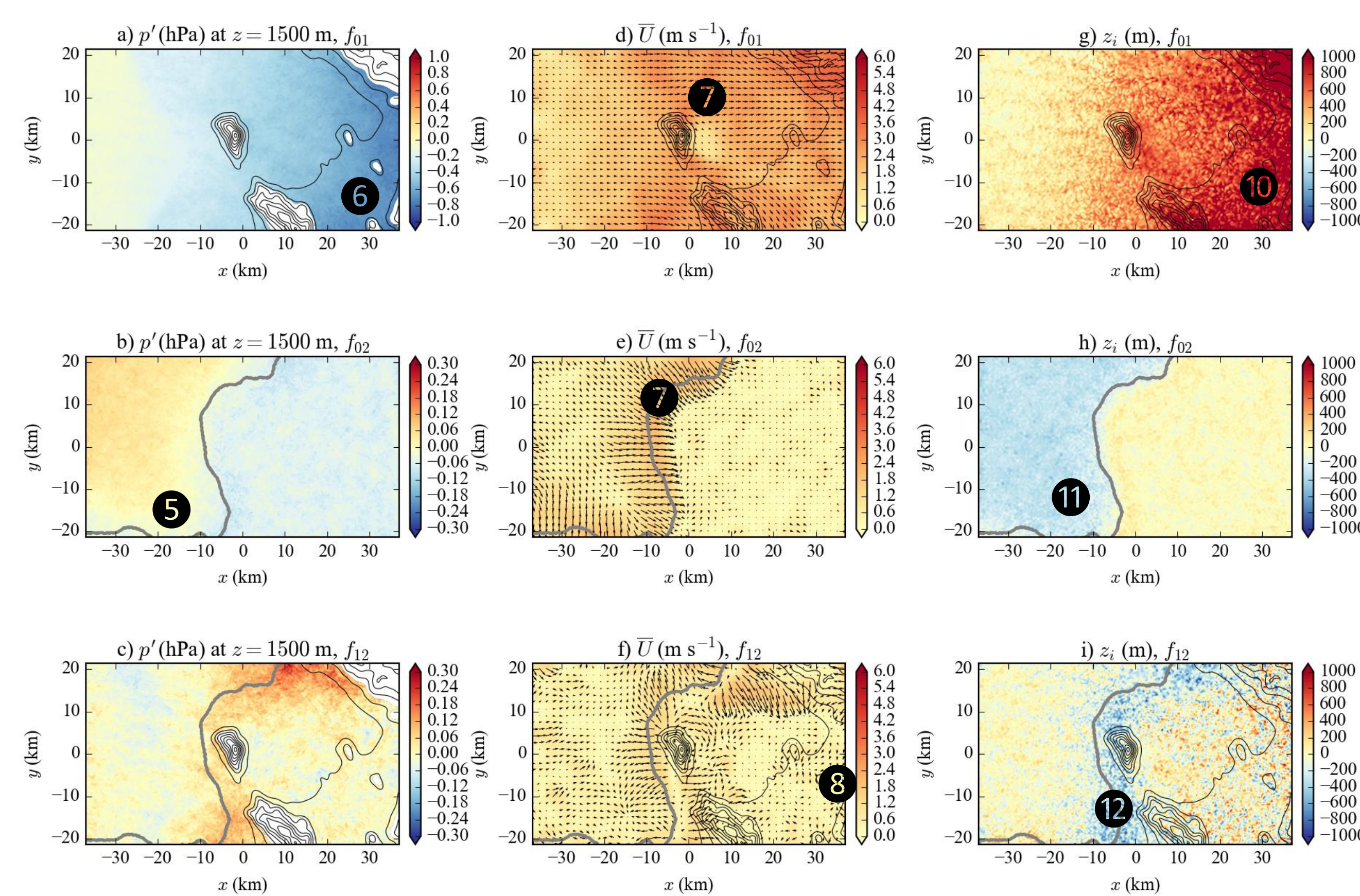
Thermal forcing is modelled by specifying a diurnal variation pattern for ΔT . Assuming that temporal variability in the longwave radiation is relatively unimportant, ΔT can be assumed to vary in time in proportion to the shortwave radiation I (e.g. using the Garnier and Ohmura, 1968, model; Z is the local solar zenith angle):

$$I = I_{max} \cos Z \Rightarrow \Delta T = \Delta T_{max} \cos Z$$

- Different values for ΔT_{max} are specified over the playa and sagebrush plain (4).
- This model leads to an enhancement of the heat flux on slopes, especially those facing SW. The heat flux is also enhanced close to the playa due to cool air advection (5). The figure on the left shows temporally averaged heat fluxes (9 hours).

Results

Maps of pressure (a-b-c), 10-m wind speed (d-e-f) and mixing height (g-h-i) factors at hour 9 (15 LST).



In the figures above, f_{01} , f_{02} and f_{12} refer to factors while s_{01} , s_{02} and s_{12} refer to simulations (see box below).

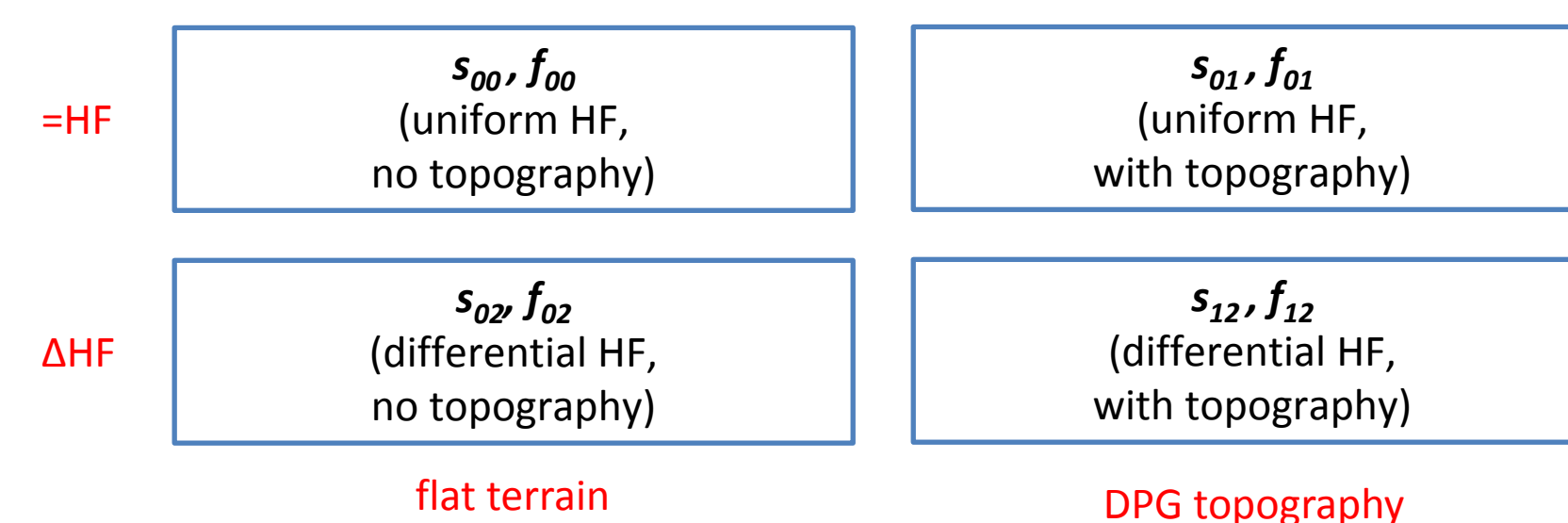
- The CBL is thinner over the playa due to weak heat fluxes 1 and thick near topography 2. Due to deeper mixing, the CBL is warmer near topography 3. Topography causes a larger horizontal temperature imbalance than differential heat fluxes 4.
- Near-surface heating causes the pressure to decrease. The pressure fall is weaker over the relatively cool playa 5. At 1500 m ASL (approx. 200 m above the playa and sagebrush plain), pressure perturbations induced by topography are larger than those induced by differential heat fluxes 6. Pressure perturbations generate breeze systems 7 (~3-4 m s⁻¹). The «inland» penetration of the breeze is strongest in the s_{12} simulation 8. Circulation induced by topographic forcing is stronger and more extensive than the playa breeze, in particular above the CBL (return flow with direction contrary to the surface breeze 9).
- The undisturbed CBL has uniform depth (parcel method). Elevated heat input related to the topography causes mixing height differences of nearly 1 km 10. Weaker heat fluxes over the playa causes mixing height differences of around 200 m 11. The interaction between topographical forcing and differential heating causes a CBL depression along the playa breeze front 12. The depression is coherent with the enhanced inland propagation of the breeze.

Factor Separation

In this study, we explore the mechanisms for CBL depth variability at DPG using the factor separation method (FS). FS (Stein and Alpert, 1993) provides a useful formalism to design sensitivity studies. Consider one phenomenon modulated by two forcing factors. Four simulations can be run: 0 (both forcings off), 1 (only forcing 1 on), 2 (only forcing 2 on), 12 (both forcings on). From each simulation one field of interest, s , is chosen (e.g., BL depth). Then four "factors" are computed:

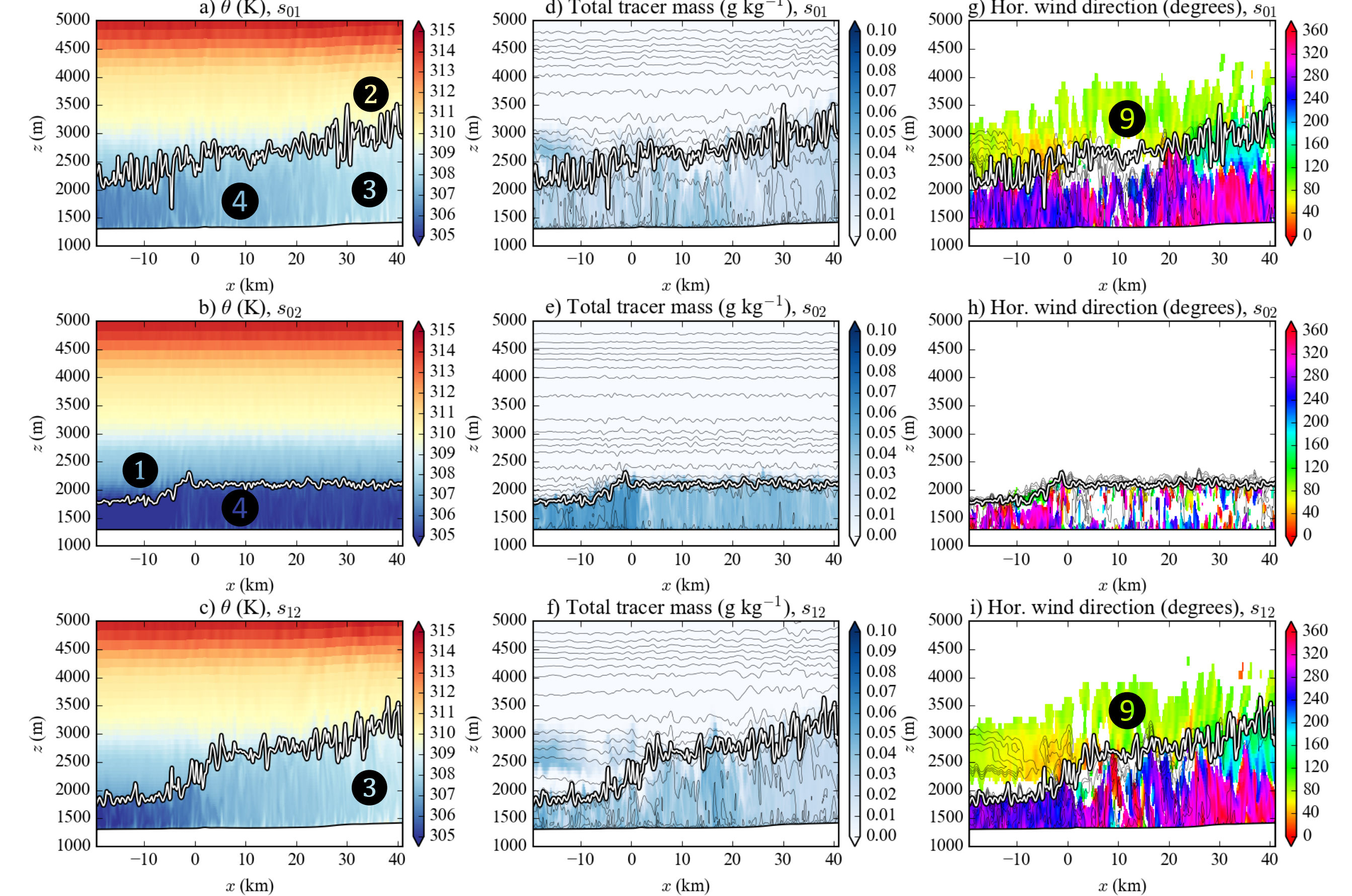
$$\begin{aligned} f_{00} &= s_{00} \\ f_{01} &= s_{01} - s_{00} \\ f_{02} &= s_{02} - s_{00} \\ f_{12} &= s_{12} - s_{01} - s_{02} + s_{00} \\ f_{00} + f_{01} + f_{02} + f_{12} &= s_{12} \end{aligned}$$

f_{00} represents the undisturbed development of a phenomenon, f_{01} and f_{02} are the pure impacts of forcings 1 and 2, f_{12} is the impact of their interaction. f_{12} represents a nonlinear interaction, manifest in the fact that $s_{12} \neq f_{00} + f_{01} + f_{02}$. In our case, forcings 1 and 2 are respectively topography and differential heat flux.



Examples of factor separation are presented in the box to the left, where f_0, f_1, f_2 and f_{12} are computed for the sensible heat flux at the surface, H (panels a-c-e-f); and in the box above.

Cross-sections of θ (a-b-c), tracer mass (d-e-f), wind direction (g-h-i) at hour 9 (15 LST).



Discussion

Why does the mixing height variability depend more on the underlying topography than on the heat fluxes?

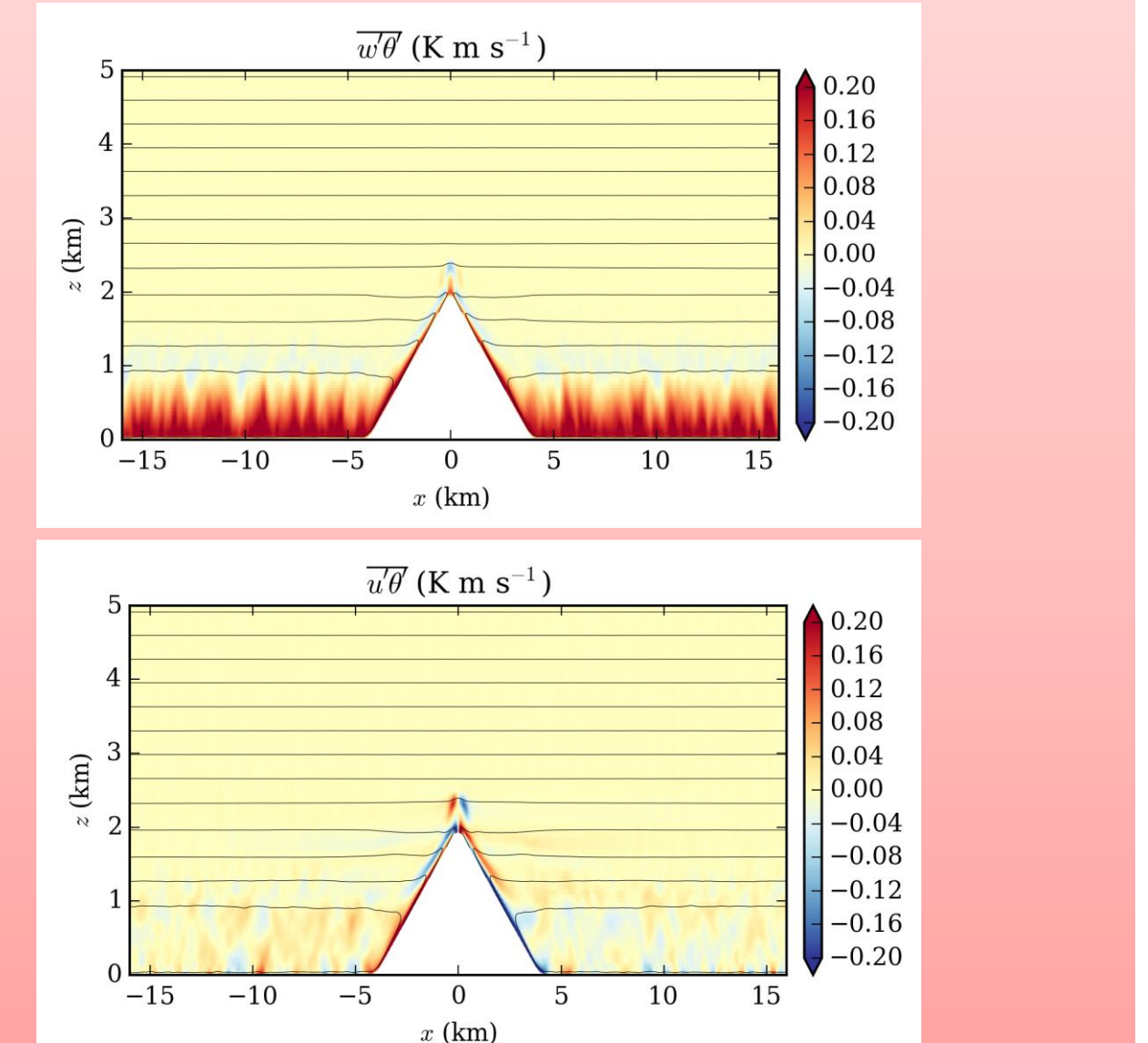
Heat engine theory (Souza et al, 2000) can give a partial explanation. According to heat-engine theory, the pressure difference between two locations at the same altitude within a dry convective circulation and the convective velocity scale are given by:

$$\Delta p = \frac{\gamma \eta}{\gamma \eta - 1 R} \frac{1}{T} c_p \Delta \theta \quad U = \sqrt{\frac{\eta}{\mu} c_p \Delta \theta}$$

Here, μ is a mechanical energy dissipation coefficient, γ is the fraction of frictional energy loss that occurs near the ground and η is a thermodynamic efficiency coefficient. Using scales for the lake breeze system and for the plain-to-mountain breeze system, these equations yield pressure-perturbation estimates respectively of -0.1 hPa and -1.4 hPa, and wind speed estimates respectively of 1 m s⁻¹ and 4 m s⁻¹, in good agreement with numerical results.

Outlook

How to study the impact of topography on the mixing height more systematically? Quasi-2D idealized simulations, aimed at: (1) developing a scaling for the mixing height near mountain ridges; (2) quantifying turbulent fluxes near mountain ridges.



References

- Bryan, and Fritsch (2002), DOI: 10.1175/1520-0493(2002)130<2917:ABFSMN>2.0.CO;2.
- Deardorff (1980), DOI: 10.1007/BF00119502
- Garnier and Ohmura (1968), DOI: 10.1175/1520-0450(1968)007<0796:AMODCT>2.0.CO;2
- Souza et al (2000), DOI: 10.1175/1520-0469(2000)057<2915:CCIBSH>2.0.CO;2
- Stein and Alpert (1993), DOI: 10.1175/1520-0469(1993)050<2107:FSINS>2.0.CO;2

Contact:

Stefano Serafin
University of Vienna
Department of Meteorology and Geophysics
Althanstraße 14 / UZA II, 1090 Vienna, Austria
stefano.serafin@univie.ac.at